Improved Methods of Characterizing Ejector Pumping Performance

Joe Der Jr.*
Northrop Corporation, Pico Rivera, California 90660

A unified method to characterize ejector pumping performance data is presented. Unlike methods used in the past where correlations are done separately for low and high flow rates or velocities, the new method can characterize ejector pumping data continuously from no flow to high primary nozzle pressure ratios. The concept of distinguishing choked and unchoked secondary ejector flow regions is introduced. In the choked-flow region, the ejector pumping characteristics are simplified in that the corrected secondary to primary weight flow ratio is a function of only the secondary to primary pressure ratio for a given ejector area ratio. Correlation of choked-flow experimental data and comparison of analytical predictions are presented. A more fundamental definition of spacing ratio is also introduced. The new spacing ratio, which characterizes the ejector mixing length by the height of the secondary flow gap instead of the nozzle diameter, is based on detailed flow mechanics of entrainment arising from the development of a free-mixing layer. Methods and theories presented are demonstrated and verified using available data. Rectangular or two-dimensional ejector data are also used in the choked-flow region correlation.

Nomenclature

A = area
D = diameter
L_S = ejector shroud (mixing) length
P = static pressure
P_t = total pressure
T_t = total absolute temperature
u' = main stream or longitudinal velocity component
U' = free-mixing layer or boundary-layer outer edge velocity
w' = crossflow or transverse velocity component
W = flow rate
x' = longitudinal distance
z' = transverse distance
τ = T_{ts}/T_{tp}
ω = W_s/W_p
δ = boundary- or mixing-layer thickness
Δ = secondary flow gap distance
ϵ = ejector divergence angle

Subscripts

E = entrainment
L = leakage
p = primary flow
s = secondary flow
0 = ambient

Introduction

THE use of ejectors on various aircraft subsystems has been common for many years. As an air pumping device, the advantages of an ejector are its simplicity, light weight, freedom from moving parts, and reliability. An important application of ejectors is thrust augmentation.

Numerous theoretical and experimental investigations of ejectors have been conducted. Some well-known experimental results were published over 30 years ago. Data on circular ejectors with constant mixing area were published by Greathouse and Hollister[1] in 1953 and by DeLeo and Wood[2] in 1952–1958. A popular theoretical method in use currently is the work presented by Anderson[3,4] in 1974. However, the REJECT computer code of Anderson is only applicable for supersonic choked-flow ejectors. While the application of ejectors has been extensive, with a large volume of available experimental data, little attention has been directed toward a better understanding of the details of the flow mechanism and behavior. There have been no significant new advances in the method of data characterization to improve the technique of correlating experimental data. Ejector data correlations are usually separated by low and high flow rates or subsonic and supersonic flow conditions. Most ejector pumping data are still characterized in the formats of those adopted in Refs. 1 and 2.

One of the basic characteristics of ejector pumping performance is the choking point of the secondary flow, which occurs at sufficiently high primary nozzle pressure ratios. This is significant because, at the secondary flow choking point, the ejector pumping characteristics are greatly simplified. Previous studies of ejectors have ignored this point and thus led to experiments with unnecessarily large test matrices. For characterizing the minimum required or optimum ejector mixing length, the author has found that the current commonly used definition of spacing ratio (mixing length normalized by the nozzle diameter) is not universal. That is, results are only applicable for certain ejector geometries or area ratios.

In this paper, a unified and more widely applicable method of characterizing ejector pumping performance is presented. The method is demonstrated using existing experimental data.[1,2] A correlation of choked secondary flow performance, comparing experimental data from various sources and analyses using REJECT, is also presented. A more fundamental definition of ejector spacing ratio is introduced. The improved definition of spacing ratio is based on previously obscure details of free-mixing layer theory, which are directly linked to the basic mechanism of entrainment in ejector pumping. The validity of the theory is also verified using existing data.[1] Sample results of finite-difference computations[5,6] of free-mixing layer characteristics to explain the phenomenon are included. For simplicity, all information presented is for constant area mixing ejectors.

Entrainment and Free-Mixing Layer

The fundamental mechanism of ejector pumping is flow entrainment that arises from the development of a free-mixing

Presented as Paper 89-0008 at the AIAA 27th Aerospace Sciences Meeting, Reno, NV, Jan. 8–10, 1989; received March 30, 1989; revision received Dec. 12, 1989.

*Member Senior Technical Staff, Propulsion Analysis, B-2 Division, W432/UB. Associate Fellow AIAA.

layer. Although this phenomenon is well known, little has been written on the basic details. Most theoretical works[4,7] are still relying on the classical Chapman[8]-Korst[9] mixing theory, which uses the momentum integral method to solve free-mixing layer problems. The momentum integral method is limited to asymptotic or similar solutions, which are applicable only for constant pressure mixing ($dp/dx = 0$). Also, since the crossflow velocity component is not calculated, the entrainment flow rate can be determined only implicitly with a flow model exhibiting interaction between the dissipative flow region and the freestream.[10]

Explicit details of entrainment can be determined only through the complete equations of motion that include the crossflow velocity component.[5,6] Unlike the boundary layer, where boundary conditions prescribe zero crossflow velocity along the wall to compute the wall shear (skin friction), analyses of the free-mixing layer prescribe zero shear along the inner boundary, zero velocity line, and then the crossflow velocity is determined (Fig. 1). The important features here are that the crossflow is the entrainment, and the crossflow velocity along the inner boundary is the local entrainment velocity. Although it appears that the above condition violates the basic requirement for boundary-layer approximation, in that the main flow component must be much greater than the crossflow, this reversed condition is local and confined to an extremely small region. In the major portion of the free-mixing layer, the basic requirement for boundary-layer approximation still applies. One may question the accuracy since certain terms in the full equations of motion are neglected. However, the region of violation of boundary-layer assumption is local, and any error introduced is at present unknown. The level of accuracy can be determined only by comparison to experiment or complete Navier-Stokes flow computations. To the author's knowledge, no one has utilized detailed free-mixing layer solutions to compute entrainment. Nevertheless, the unknown accuracy does not invalidate the physical flow description, which is sufficient for the discussion. Therefore, similar to a boundary layer, the local entrainment rate in a free-mixing layer is directly influenced by the external flow dynamics, which include the local pressure gradient (dp/dx').

Sample finite-difference computations[5,6] of free-mixing layers with an initially separated boundary layer are shown in Figs. 2 and 3. Figure 2 shows a zero pressure gradient computation, and Fig. 3 shows a computation with zero pressure gradient applied for the first half and a gradually increasing positive pressure gradient applied for the second half. Although the samples shown here are for laminar flow, which has a much lower mixing rate, they are sufficient for demonstration. At the top of Figs. 2 and 3, main flow velocity profiles and entrained flow streamlines, which developed below the dividing streamline, are plotted. The outer edge and the inner boundary are arbitrarily defined at u'/U' values of 0.9938 and 0.0062, respectively. Points to be noted here are that along the dividing streamline, the crossflow velocity is zero, whereas along the inner boundary the crossflow velocity component, which is also the entrainment velocity, is finite. Also, results show that, with sufficient positive pressure gradient, entrainment can be reversed (negative crossflow velocity at the inner boundary) as shown in Fig. 3. Conversely, with a negative pressure gradient, the entrainment increases.[5] With zero pressure gradient ($dp/dx' = 0$), the crossflow velocity profile displayed little or no gradient, dw'/dz', near the inner boundary. Thus, despite a local violation of the boundary-layer assumption, the accuracy of the crossflow velocity, at least for zero or small pressure gradient laminar flows, is expected to be valid even along the inner boundary. It is clear, therefore, from results shown in Figs. 2 and 3, that ejector pumping is a result of entrainment and that the entrainment takes place along the inner boundary or the zero velocity line of the free-mixing layer, having a direction normal to the main flow.

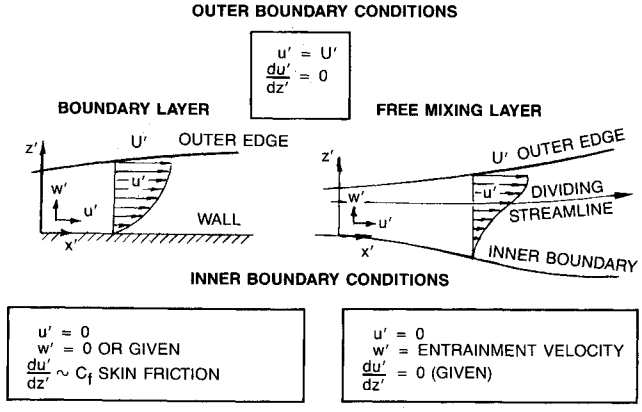

Fig. 1 Boundary conditions comparison between boundary layer and free-mixing (shear) layer.

Spacing Ratio and Optimum Mixing Length

A successful ejector design requires the selection of a proper spacing ratio, which has been commonly defined as the mixing length normalized by the primary nozzle diameter. The mixing length is defined as the distance measured from the trailing edge of the primary nozzle to the end of the ejector (Fig. 4).

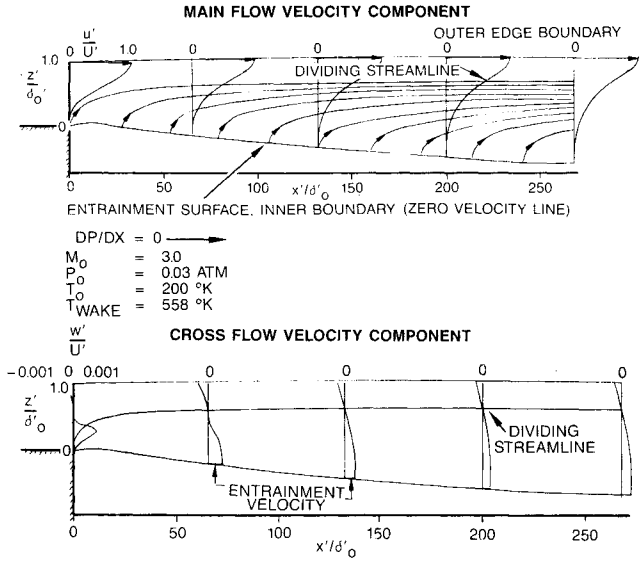

Fig. 2 Finite-difference calculation of free-mixing layer (laminar flow with zero pressure gradient).

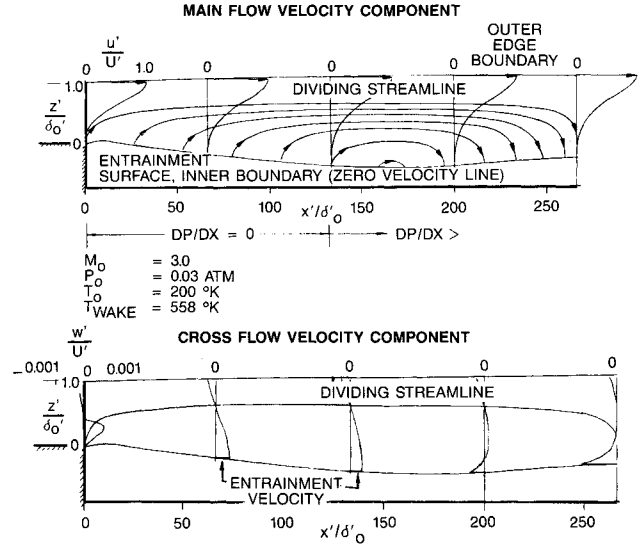

Fig. 3 Finite-difference calculation of free-mixing layer (laminar flow with zero and positive pressure gradients).

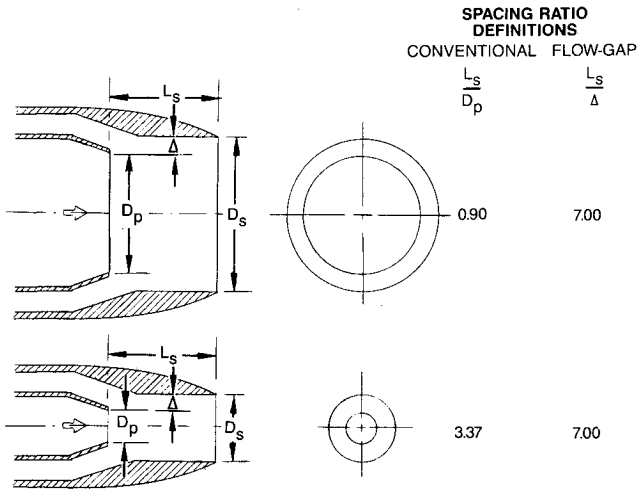

Fig. 4 Comparison of ejector spacing ratio definitions.

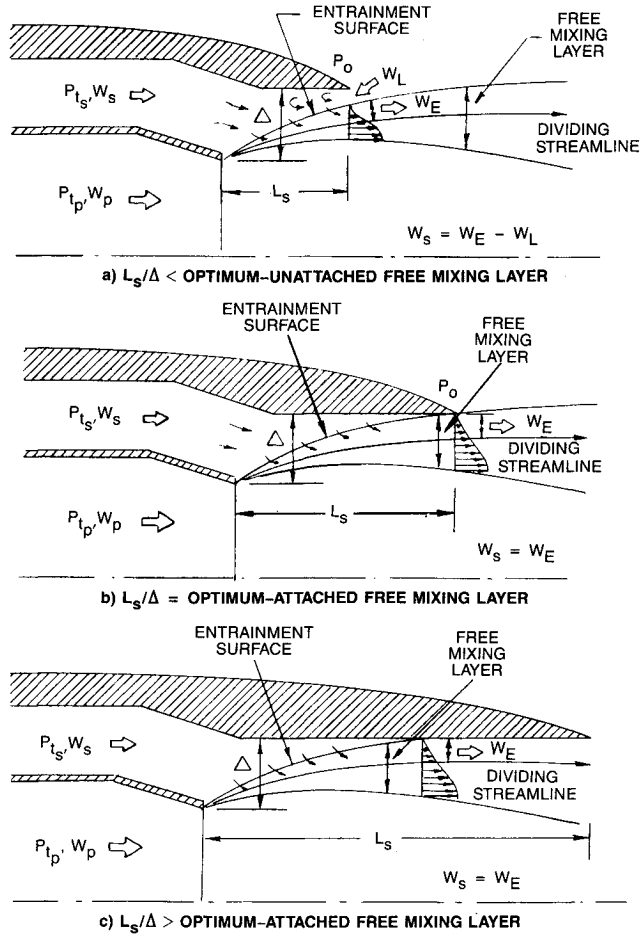

Fig. 5 Correlation of free-mixing layer attachment and optimum ejector mixing length.

Based on the flow details of entrainment in free-mixing layer development described above, it is reasonable to postulate that a more fundamental normalizing parameter is one that can be directly related to the free-mixing layer development instead of the size of the primary jet. Since the flow gap distance Δ between the primary nozzle and the ejector shroud is directly controlling the height of the free-mixing layer development, it would be, therefore, a more meaningful parameter. A comparison of the commonly used and the new introduced spacing ratio definitions is shown in Fig. 4 for two circular ejector configurations. Although ejector area ratios of the two ejector

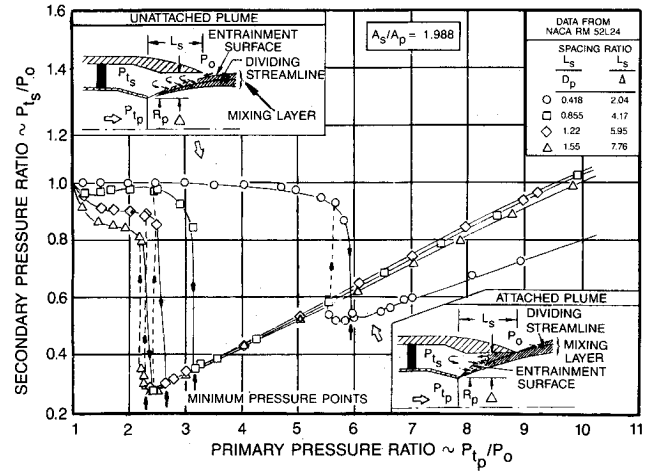

Fig. 6 Entrained flow characteristics of ejector with zero secondary flow.

configurations are different, the free-mixing layer development is similar because the spacing ratios L_s/Δ are equal. On the other hand, their spacing ratios, by the commonly used definition, L_s/D_p, are quite different.

By the same physical reasoning, the minimum required mixing length for optimum ejector pumping would be one that must be long enough to provide free-mixing layer attachment as demonstrated in Figs. 5a–5c. Figure 5a shows an unattached free-mixing layer with an inadequate mixing length; and, therefore, entrained air can be flowing or leaking from outside the ejector. In Fig. 5b, the ejector length is just long enough to achieve free-mixing layer attachment; and, therefore, the entrainment or pumping is confined to the secondary flow. However, in Fig. 5c, the mixing length (ejector shroud) is longer than required for free-mixing layer attachment, but since the additional mixing length does not contribute to any increase of entrainment area, no improvement in ejector pumping can be realized.

The improvement in using the secondary flow gap instead of the nozzle diameter for normalizing the mixing length can be verified by data presented in Ref. 1. In Ref. 1, secondary vs primary pressure ratios were presented for various spacing ratios and area ratios for the no secondary flow condition ($W_s = 0$). Figure 6 shows samples of data presented in Ref. 1 for a series of four spacing ratios with a constant ejector area ratio A_s/A_p. At low primary nozzle pressure ratios, the expansion of the jet was insufficient to attach the free-mixing layer; and, thus, the secondary pressure P_{t_s} remains nearly equal to that of the ambient, i.e., $P_{t_s}/P_0 = 1.0$. As the nozzle pressure ratio increases, the free-mixing layer attaches, which then causes the secondary pressure to drop rapidly due to flow entrainment. With the information presented, one can now correlate the mixing length required for a free-mixing layer attachment as a function of minimum primary nozzle pressure ratio, by selecting the nozzle pressure ratios at the points of minimum secondary pressure, as depicted in Fig. 6. In the region of the rapid drop of secondary pressure, the jet was expanding like a convergent-divergent nozzle. Also, due to hysteresis phenomenon, when the primary nozzle pressure was reduced from high to low levels, the free-mixing layer detached at a lower nozzle pressure ratio than that at the attachment point. The reversed throttling curves are shown in Fig. 6 as dotted lines.

Figures 7 and 8 compare correlations of ejector spacing ratio with minimum required primary pressure ratio for free-mixing layer attachment for zero secondary flow data presented in Ref. 1. Since data were presented for four ejector area ratios, four curves also result in Fig. 7 for the commonly used definition, for each of the curves correlates only for a specific ejector area ratio. Figure 8 shows the same correlation but for the redefined spacing ratio, normalized by flow gap Δ.

Unlike the results shown in Fig. 7, the data in Fig. 8 collapsed into a single curve, which strongly indicates that the data are independent of the ejector area ratio A_s/A_p. Although the correlation shown in Fig. 8 is only for zero secondary flow condition, little variation is expected for finite secondary flow due the steep transition slopes displayed in Fig. 6. For finite secondary flow conditions, the secondary pressure is expected to increase, riding along the transition portion of the curves. It can be concluded that the preceding correlation verified that the ejector entrainment is indeed a free-mixing layer flow phenomenon, and for sizing of an ejector, the mixing length should be fundamentally characterized by the flow gap Δ, instead of the diameter of the primary or secondary nozzle.

The definition of secondary flow gap for other geometries can be similarly defined based on the principle of height allowance for free-mixing layer development. Sample geometries are shown in Fig. 9. For a rectangular or two-dimensional nozzle (Fig. 9a), the ejector flow gap is defined much like that for a circular jet. Due to the tendency of a rectangular plume to develop into an axisymmetric shape,[11] however, extra allowance should be given to the spacing ratio along the edge of the ejector, because the local plume expansion angle there will be smaller. For cluster nozzle ejectors such as those shown in Figs. 9b and 9c, a reasonable secondary flow gap definition would be the maximum distance between adjacent nozzles or nozzle to ejector shroud. For cluster nozzle ejector, overlappings of adjacent plumes are required to allow for total mutual attachment of mixing layers.

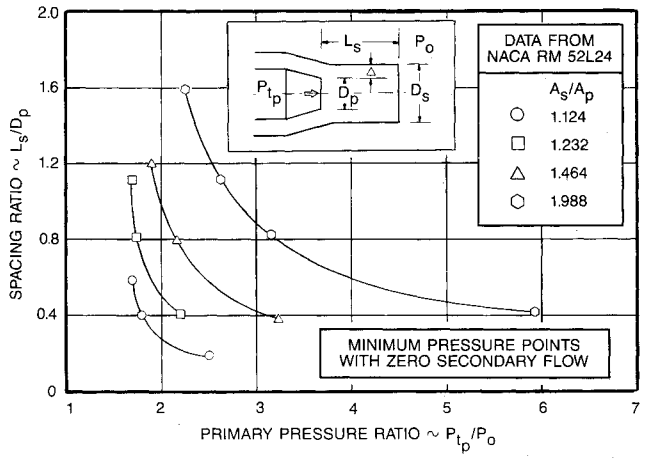

Fig. 7 Correlation of minimum ejector spacing ratio—mixing length normalized by nozzle diameter.

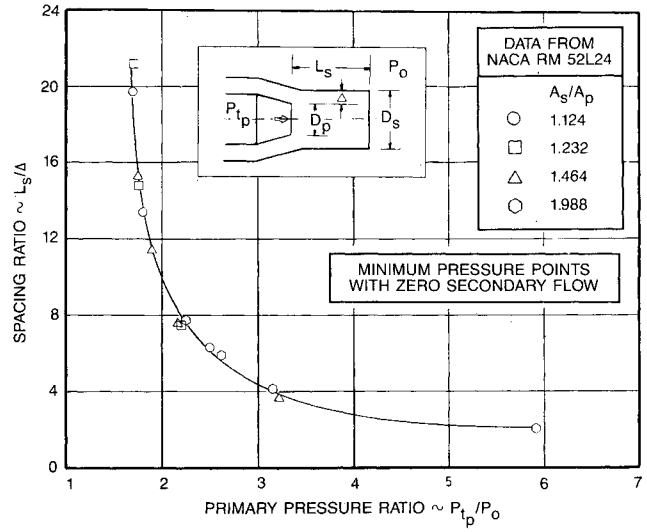

Fig. 8 Correlation of minimum ejector spacing ratio—mixing length normalized by secondary flow gap Δ.

Although the current study was limited to constant mixing areas, or zero ejector divergence angle ($\epsilon = 0$), data can be similarly correlated for ejectors with finite divergence angles ($\epsilon > 0$). For ejectors with finite divergence angles, the mixing length and ejector flow gap can be similarly defined as shown in Fig. 9d, where distances, as in the case for constant mixing area ejectors, are also measured parallel and perpendicular to the internal surface of the ejector shroud. Thus, to extend the present correlation as shown in Fig. 8, a family of constant ejector divergence angles can be generated using systematically obtained experimental data.

Unified Method of Characterization

Current common methods of characterizing ejector pumping data plot the secondary or corrected secondary weight flow ratio vs either the primary or the secondary pressure ratio, formats similar to those presented in Refs. 1 and 2. In this section an improved method is introduced. Advantages and important physical characteristics will be discussed and demonstrated using the existing data of Refs. 1 and 2.

An important characteristic of ejector flow is secondary flow choking. With adequate primary nozzle pressure ratio, the secondary flow is choked from simultaneous flow acceleration by entrainment and flow passage area squeezed by the primary jet expansion. This point is significant because in secondary flow choking, the corrected secondary to primary weight flow ratio is a function of only the secondary to primary pressure ratio for a given ejector area ratio.[3] Another significant point is that results from circular ejectors are also applicable for ejectors of various shapes, such as two-dimensional or rectangular. Secondary choked-flow characteristics and correlation are discussed in the next section.

A unified method of characterizing the ejector pumping performance is shown in Fig. 10. Here, the secondary to pri-

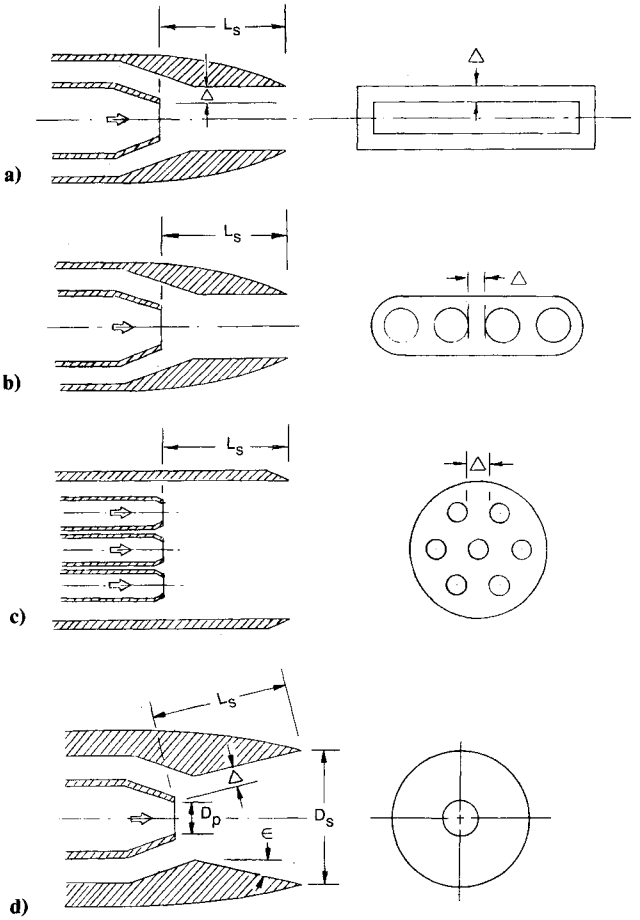

Fig. 9 Secondary flow gap and mixing length definitions for various ejector geometries.

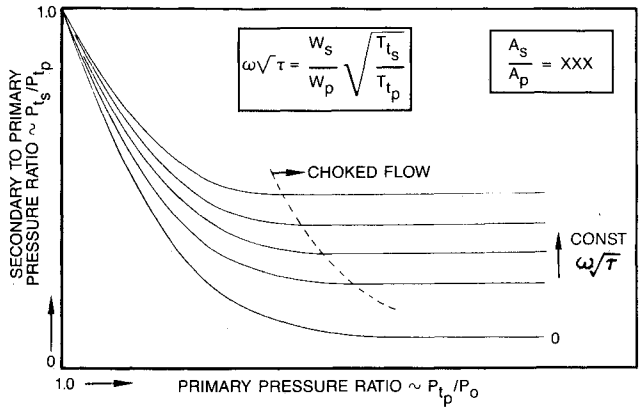

Fig. 10 Unified plot to characterize ejector pumping performance.

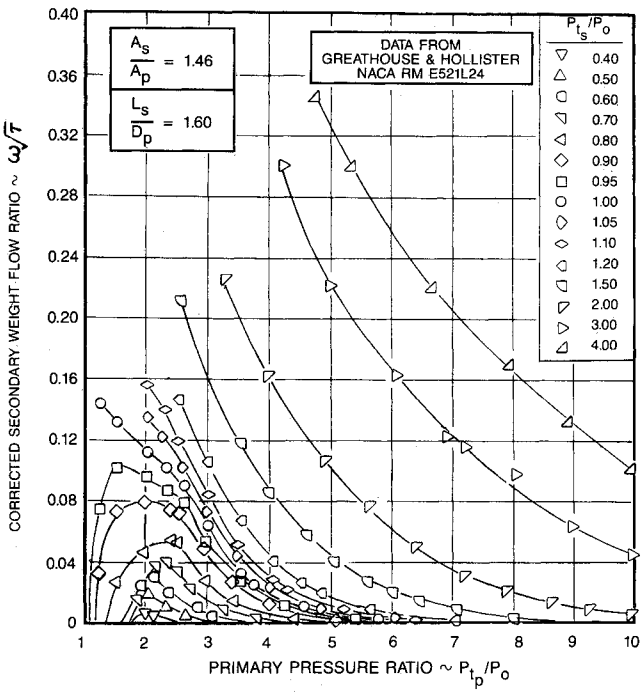

Fig. 11 Ejector pumping data as presented by Greathouse and Hollister.[1]

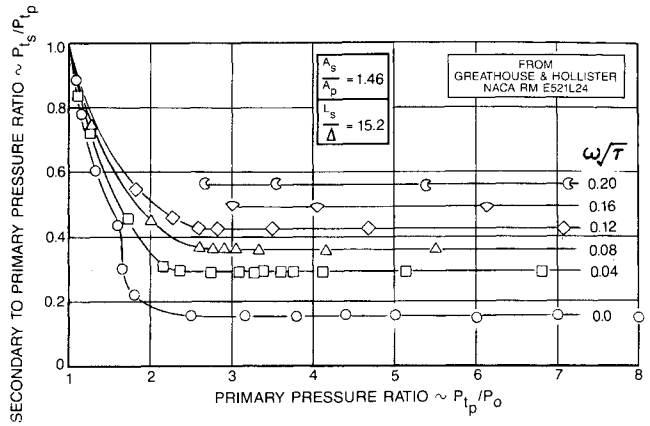

Fig. 12 Interpolated and replotted ejector pumping data of Greathouse and Hollister.[1]

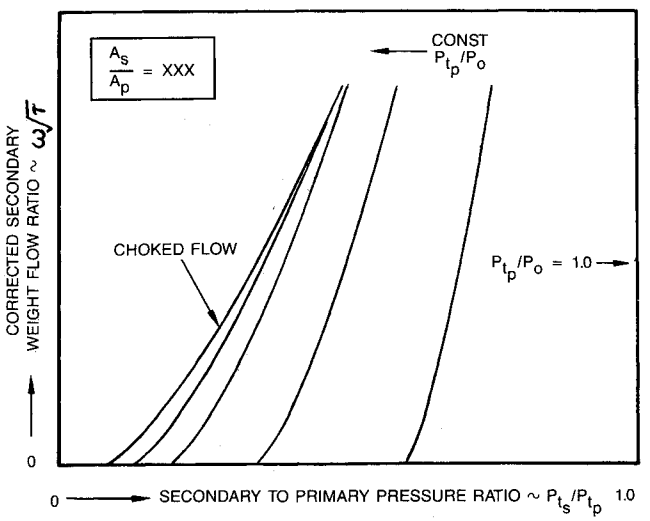

Fig. 13 Ejector pumping characteristics (cross-plot of Fig. 10).

mary pressure ratio is plotted against the primary nozzle pressure ratio for constant values of corrected secondary to primary weight flow ratio. At high primary nozzle pressure, the secondary flow is choked, indicated by the horizontal lines or constant values of secondary to primary pressure ratio. In the unchoked-flow region, all curves converge toward the point of secondary to primary pressure ratio of 1.0 at zero primary flow condition ($P_{t_p}/P_0 = 1.0$). In this format the characteristics between extreme low and high ejector flows are continuous and determinate. In the format adopted by Greathouse and Hollister,[1] which plotted the corrected secondary weight flow ratio vs the primary pressure ratio for constant secondary pressure ratio, the secondary weight flow ratio is indeterminate at $P_{t_p}/P_0 = 1.0$. A sample of the data, as presented in Ref. 1, is shown in Fig. 11. The reason for the indeterminacy of the data at $P_{t_p}/P_0 = 1.0$ in Fig. 11 is that when the curves are plotted for constant secondary pressure ratio, a pseudo-singularity in weight flow ratio is created. In principle, by L'Hospitals' rule, a limiting condition of weight flow ratio exists at the no flow condition because as the primary nozzle pressure decreases, both W_s and W_p are also decreasing until they approach zero at $P_{t_p}/P_0 = 1.0$. However, this limiting condition must be accompanied by the simultaneous approaches of equal secondary and primary pressures ($P_{t_s}/P_{t_p} = 1.0$), a condition that a constant secondary pressure curve cannot represent.

Figure 12 shows an interpolation and replot of the Greathouse and Hollister data of Fig. 11 into the format of Fig. 10. In comparison to the original data, Fig. 12 shows curves of a well-behaved family, and the regions of choked and unchoked secondary flows are identifiable by the constant (horizontal) and variable portions of the curves. In the low primary nozzle pressure region, all curves are determinate and converging toward $P_{t_s}/P_{t_p} = 1.0$ exactly. In the orginal plot of Fig. 11, constant secondary pressure curves are diverging in the directions of plus or minus infinity. The extra bump at the knee of the constant $\omega\sqrt{\tau} = 0$ curve in Fig. 12 (near $P_{t_p}/P_0 = 1.7$) is attributed to the sudden suction due to entrainment within the closed secondary flow channel when the free-mixing layer first attaches (see Fig. 6). It should be mentioned that although the plot format shown in Figs. 10 and 12 can be implied directly from the one-dimensional flow theory,[2,13,14] no detailed discussion to highlight the important characteristics of the ejector pumping curves had been presented. Previous works,[13,14] for example, did not take advantage of the limiting value at the no flow condition ($P_{t_p}/P_0 = 1.0$) for more accurate data characterization at the extreme low primary nozzle flow conditions.

In practice, it is also useful to cross-plot the ejector performance data as shown in Fig. 10 or Fig. 12 into the form shown in Fig. 13, where the corrected secondary to primary weight flow ratio is plotted against the secondary to primary pressure ratio for constant primary nozzle pressure ratio. Here, the vertical line at the far right, $P_{t_s}/P_{t_p} = 1.0$, corresponds to the point of zero primary and secondary flow (i.e.,

$P_{t_p}/P_0 = 1.0$). As the primary nozzle pressure increases, the line moves toward the left until the secondary flow is choked. Beyond the choked point, all higher nozzle pressure ratio lines will be stacked on top of the choked flow line. This data format is more appropriate for choked flow data characterization because only a single curve is needed to represent the performance for each ejector area ratio. Figure 14 shows a replot of the Greathouse and Hollister data in Fig. 11 into the format shown in Fig. 13. Since the data point conversion here is one for one, the massive piling of data in a small region indicated that a major portion of the experiments was conducted along the choked flow line. If the present method of characterization had been adopted, the test matrix could have been greatly economized and optimized for a much broader coverage.

Similar transformation of the DeLeo and Wood data of Ref. 2 was also performed, and comparisons are shown in Figs. 15 and 16. In this series of experiments, data were obtained for a constant ejector spacing ratio L_s/D_s (mixing length normalized by the ejector diameter) of 7.5. Figure 15 shows sample data, as presented in Ref. 2, where corrected secondary weight flow is plotted against the secondary pressure ratio for constant primary pressure ratios. The interpolated and extrapolated results are shown in Fig. 16. As in the results when using the data of Ref. 1, Fig. 16 clearly reveals the regions of choked and unchoked secondary flows, and all curves are smoothly converging toward the no flow ($P_{t_p}/P_0 = 1.0$) condition. Unlike the original curves shown in Fig. 15, Fig. 16 displays data trends of families of curves, which vary consistently and uniformly. Ejector spacing ratios, as characterized by the flow gap, Δ, are also transformed and shown in each of the data plots presented in Fig. 16. In the context of the new spacing ratio definition, the mixing lengths of ejectors tested by DeLeo and Wood are long, with a spacing ratio of up to 165 for the smallest ejector area ratio ($A_s/A_p = 1.21$).

Choked-Flow Characteristics

As mentioned earlier, at high primary nozzle pressure ratios, the secondary flow becomes choked, and the corrected secondary to primary weight flow ratio is only a function of the secondary to primary pressure ratio for a given geometry. A theoretical computer code, designated as REJECT, was presented by Anderson.[3,4] The code combined the method of characteristics for supersonic jets and the momentum integral mixing theory of Korst[9] to obtain solutions of supersonic ejector performance. Since the jet flowfield is limited to supersonic flows and only gross entrainment flow properties are obtained from the momentum integral theory, solutions are limited to choked secondary flows.

Ejector pumping performance based on REJECT[3,4] is shown in Fig. 17, where corrected secondary weight flow ratio is plotted against ejector area ratio for constant values of secondary to primary pressure ratios. This format is useful for the sizing of ejectors for given flow requirements. Results from one-dimensional flow theory[2] are also shown in Fig. 17 as a dotted line for comparison. In general, one-dimensional

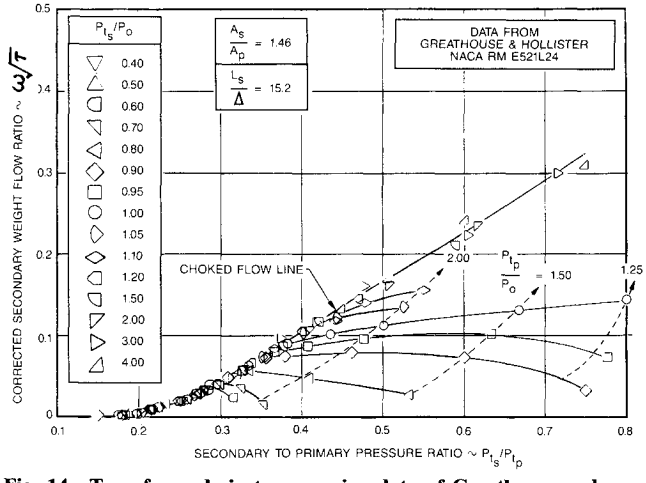

Fig. 14 Transformed ejector pumping data of Greathouse and Hollister.[1]

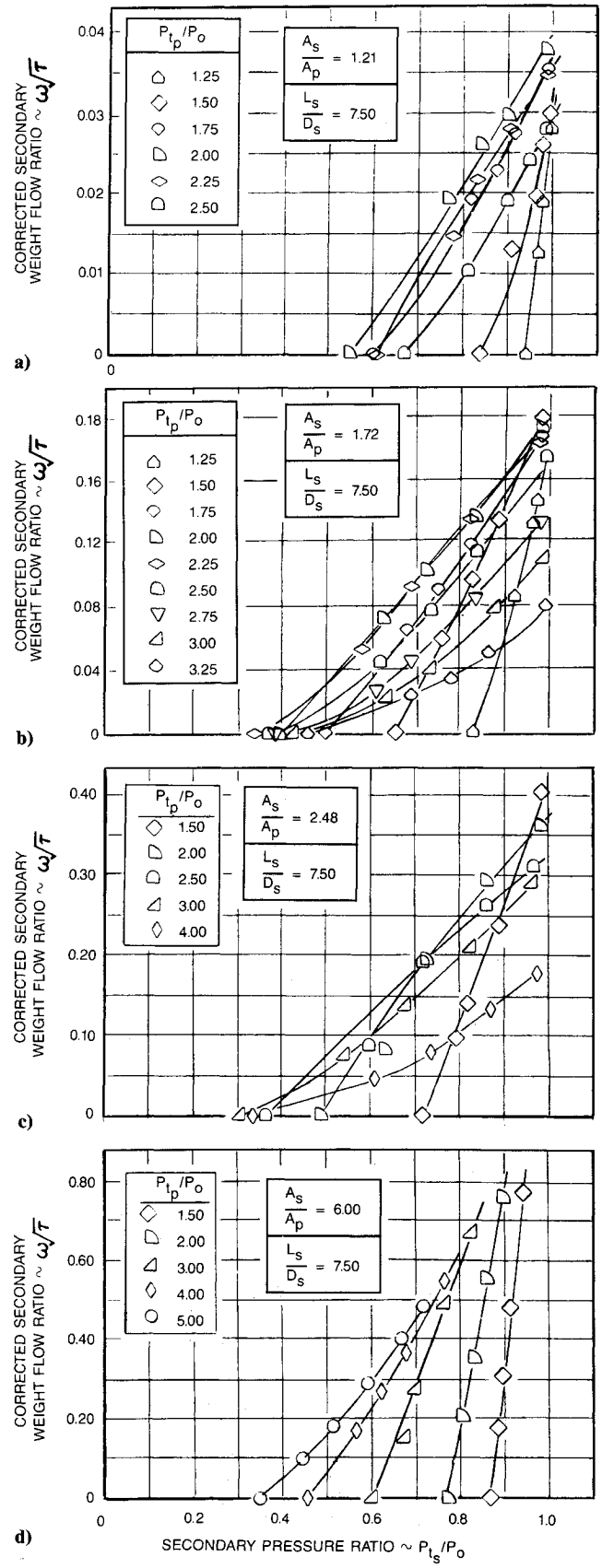

Fig. 15 Ejector pumping data as presented by DeLeo and Wood.[2]

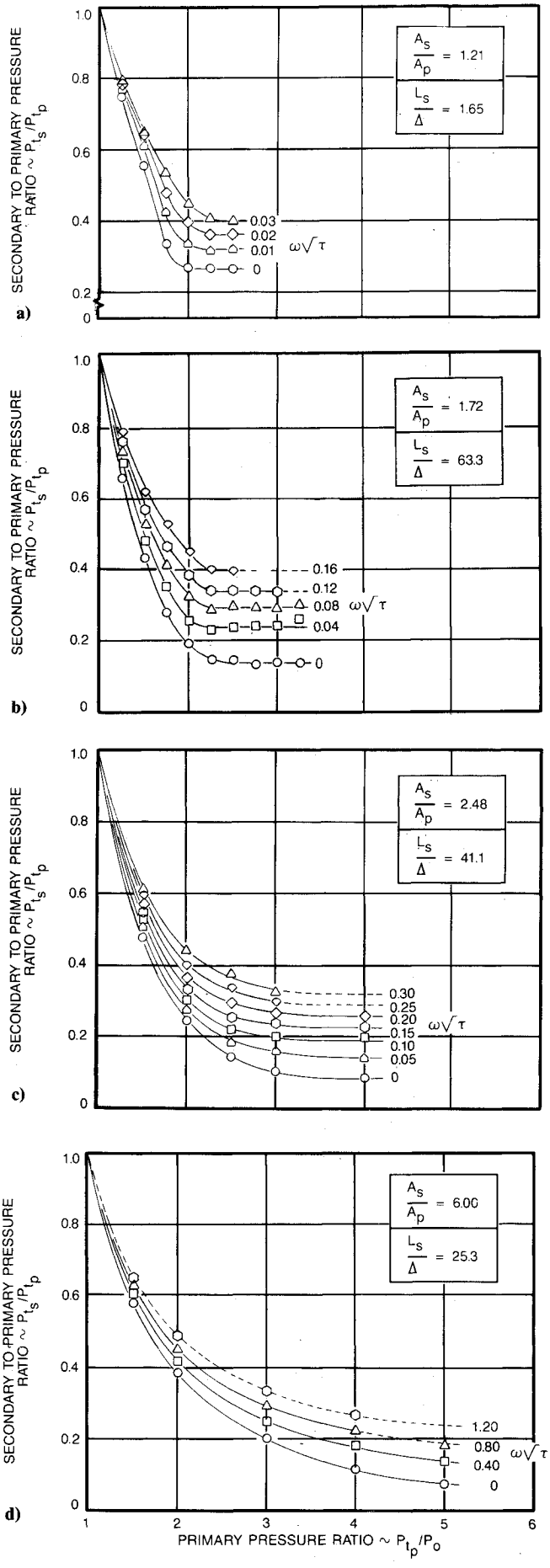

Fig. 16 Interpolated and replotted ejector pumping data of DeLeo and Wood.[2]

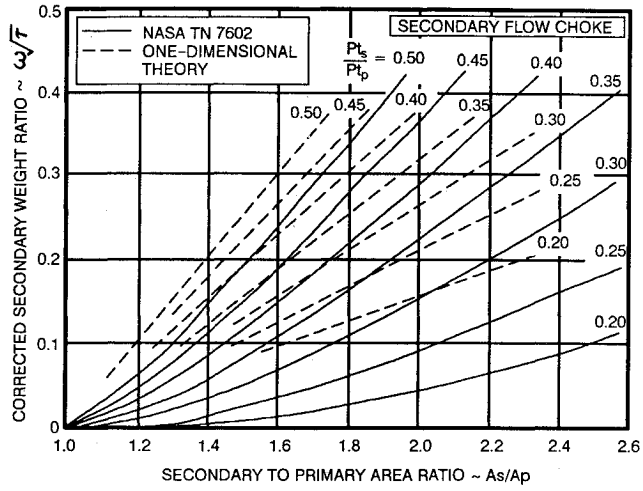

Fig. 17 Analytical prediction of ejector pumping performance.

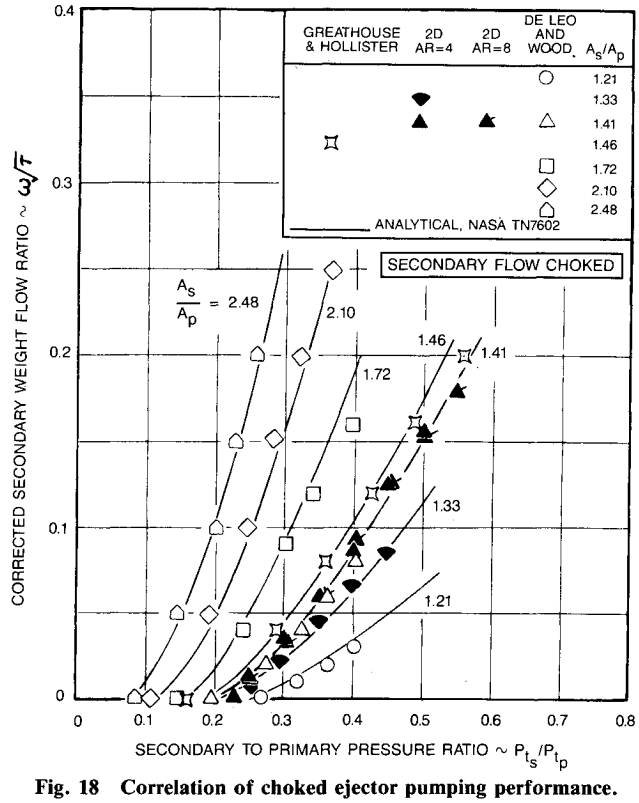

Fig. 18 Correlation of choked ejector pumping performance.

flow theory overpredicts choked secondary flow ejector pumping rate.

Figure 18 shows a comparison between the analytical prediction of REJECT and choked-flow experimental data.[1,2] Included also are two-dimensional data from Ref. 15 for two rectangular ejectors with aspect ratios of 4 and 8, respectively. The agreement between prediction and experimental data is excellent, including the two-dimensional nozzle ejector data. The excellent agreement between circular and two-dimensional ejectors, with aspect ratios of up to 8, implies that for choked ejector operation, the ejector pumping rate is dependent only on the effective area ratio. More experimental data, such as those for cluster nozzles shown in Figs. 9b and 9c, should be compared before the above conclusion is finalized.

Conclusions

An improved method to characterize ejector pumping data has been presented. The method, which is universal, provides a consistent and unified approach to obtaining, analyzing, and correlating future and existing experimental data. The ability

to distinguish choked and unchoked secondary flow regions provides future investigators with better insight to the problem both experimentally and theoretically. In the secondary flow choked region, the ejector pumping characteristics are simplified in that the corrected secondary to primary weight flow ratio is only a function of the secondary to primary pressure ratio. Correlation of choked flow data indicated that results from circular ejectors are also applicable to nonaxisymmetric ejectors such as two-dimensional or rectangular ejectors.

An improved and more fundamental definition of ejector spacing ratio has also been introduced. A close examination of the details of flow entrainment in free-mixing layer theory not only led to a more fundamental method to characterize ejector mixing length; it also sheds light on the understanding of the basic ejector flow entrainment process.

Acknowledgments

This paper was written under the sponsorship of Non-Contractual Technical Activity (NCTA). The author wishes to acknowledge suggestions given by M. Yomada, B. Forrette, M. Kontos, and D. Lotz.

References

[1]Greathouse, W. K., and Hollister, D. P., "Air-Flow and Thrust Characteristics of Several Cylindrical Cooling-Air Ejectors with a Primary to Secondary Temperature Ratio of 1.0," NACA Lewis Flight Prop. Lab., Cleveland, OH, NACA RM E521L24, March 1953.

[2]DeLeo, R. V., and Wood, R. D., "An Experimental Investigation of the Use of Hot Gas Ejectors for Boundary Layer Control," Wright Air Development Center, Wright-Patterson AFB, OH, WADS TR 52-128, Pt. I, April 1952, Pt. II, Dec. 1953, Pt. III, June 1958.

[3]Anderson, B. H., "Assessment of an Analytical Procedure for Predicting Supersonic Ejector Nozzle Performance," NACA Lewis Research Center, Cleveland, OH, NASA TN-D-7601, April 1974.

[4]Anderson, B. H., "Computer Program for Calculating the Flow Field of Supersonic Ejector Nozzles," NACA Lewis Research Center, Cleveland, OH, NASA TN-D-7602, April 1974.

[5]Der, J., Jr., "A Numerical Method for Analyzing Two-Dimensional Compressible Free-Mixing Layer Problems," Master's Thesis, Dept. of Engineering, U.C.L.A., Los Angeles, CA, 1965.

[6]Charwat, A. F., and Der, J., Jr., "Studies on Laminar and Turbulent Free Shear Layers with a Finite Initial Boundary Layer at Separation," *Proceedings of Specialists' Meeting on Separated Flows*, Rhode-Saint-Genèse, Belgium, May 10–13, 1966, sponsored by AGARD Fluid Dynamics Panel, NATO, Paris, France.

[7]Bauer, R. C., "A Method for Estimating Jet Entrainment Effects on Nozzle-Afterbody Drag," Arnold Engineering Development Center, Tullahoma, TN, AEDC TR-79-85, Oct. 1979.

[8]Chapman, D. R., "Laminar Mixing of a Compressible Fluid," Ames Aero. Lab., Moffett Field, CA, NACA Rept. 958, 1950.

[9]Korst, H. H., and Chow, W. L., "Non-Isoenergetic Turbulent ($Pr_t = 1$) Jet Mixing Between Two Compressible Streams at Constant Pressure," NASA CR-419, 1966.

[10]Crocco, L., and Lee, L., "A Mixing Theory for the Interaction Between Dissipative Flows and Nearly Isentropic Streams," *Journal of Aeronautical Science*, Vol. 19, No. 10, 1952, pp. 649–676.

[11]Chu, C. W., Der, J., Jr., and Wun, W., "Simple Two-Dimensional Nozzle Plume Model for Infrared Analysis," *Journal of Aircraft*, Vol. 18, No. 12, 1981, pp. 1038–1043.

[12]Chow, W. L., and Addy, A. L., "Interaction Between Primary and Secondary Streams of Supersonic Ejector Systems and Their Performance Characteristics," *AIAA Journal*, Vol. 2, No. 4, 1964, pp. 685–695.

[13]Brooke, D., Dusa, D. J., Kuchar, A. P., and Romine, B. M., "Initial Performance Evaluation of 2DCD Ejector Exhaust Systems," AIAA Paper 86-1615, June 1986.

[14]Federspiel, J. F., and Kuchar, A. P., "Performance Evaluation of a Two-Dimensional Convergent-Divergent Ejector Exhaust System," AIAA Paper 88-2999, July 1988.

[15]Anon., Northrop Ventura Div., Ventura, CA, Rept. NVR 78-61, 1978.